

Figure 1: Blue line is the time signal of δp_e from IAW simulation with $T_i = 0.2T_e$. Red line shows a mode damping trend with a rate calculated from (3.2). The time unit $\tau_0 = 1/\omega_0$.

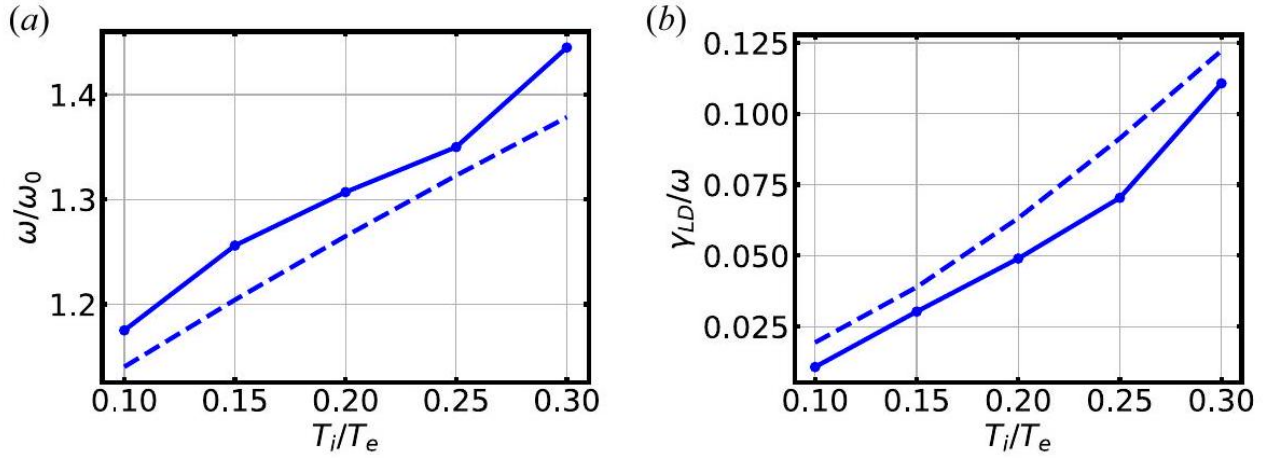


Figure 2: Frequencies (a) and damping rates (b) from IAW simulation for different values of T_i/T_e . The dashed lines are the theoretical results calculated from (3.1) and (3.2).

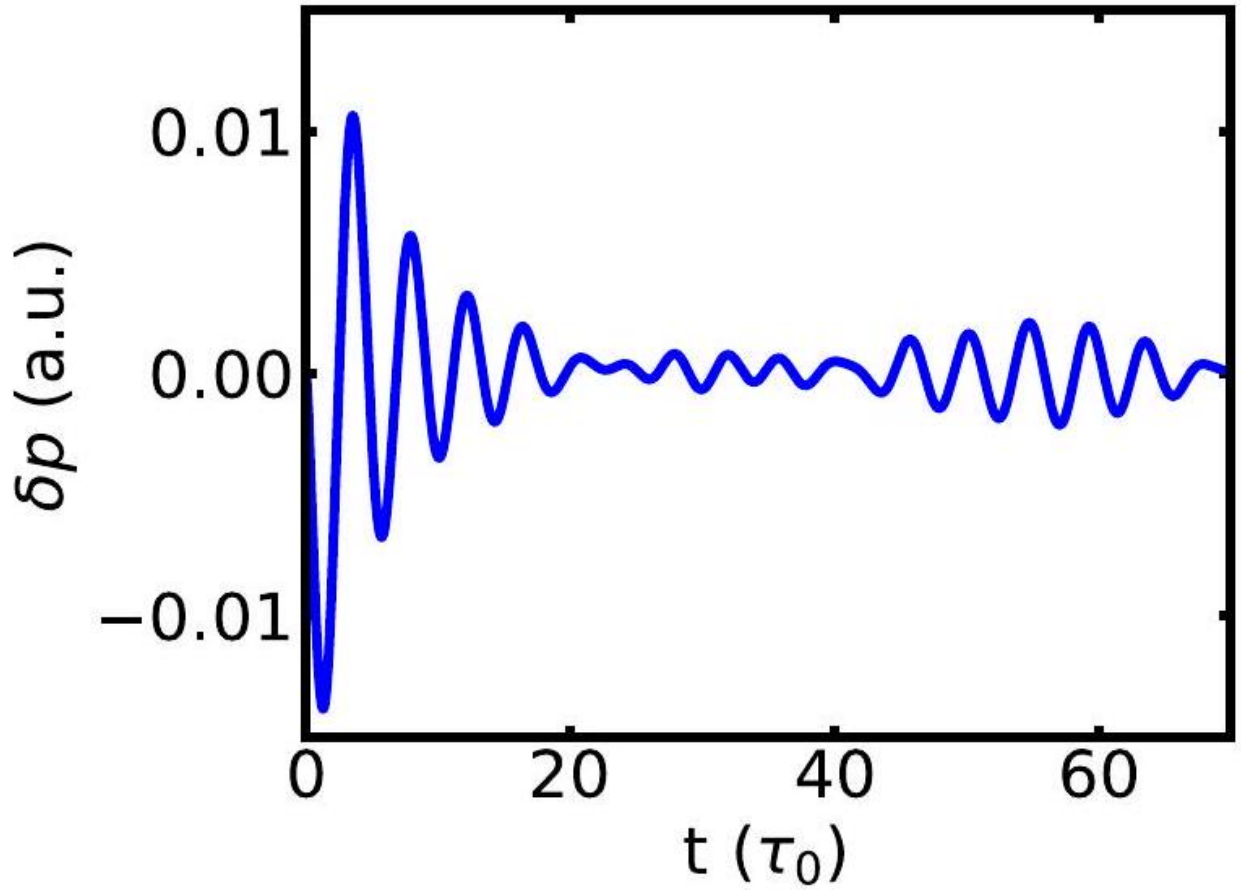


Figure 3: Time evolution of δp_e from IAW simulation with $T_i = 0.3T_e$, showing echoes of oscillation after the mode is damped.

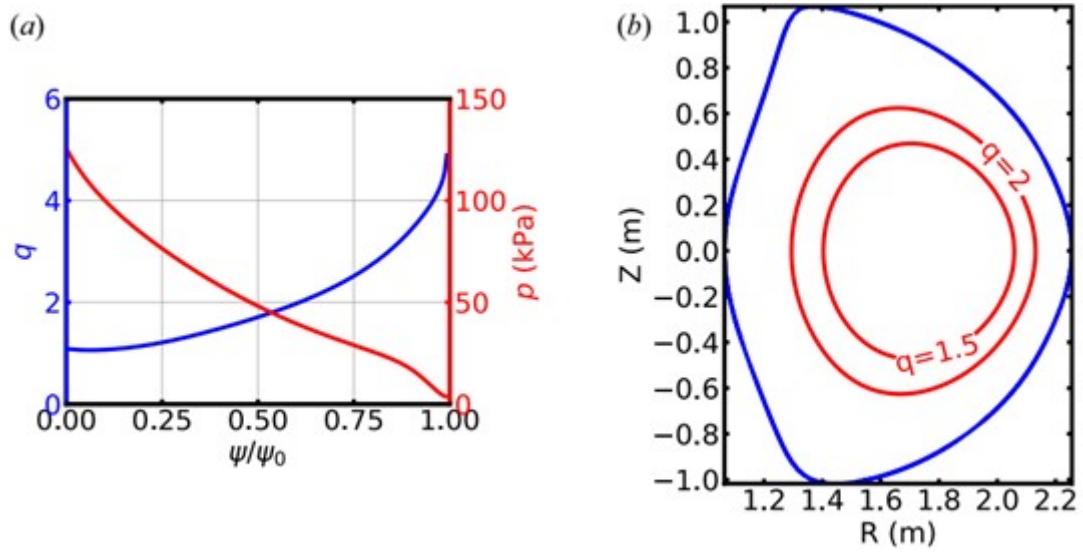


Figure 4: (a) Profiles of q and total pressure of the equilibrium used in the DIII-D simulation. (b) Flux contours and mesh boundary used in the simulation.

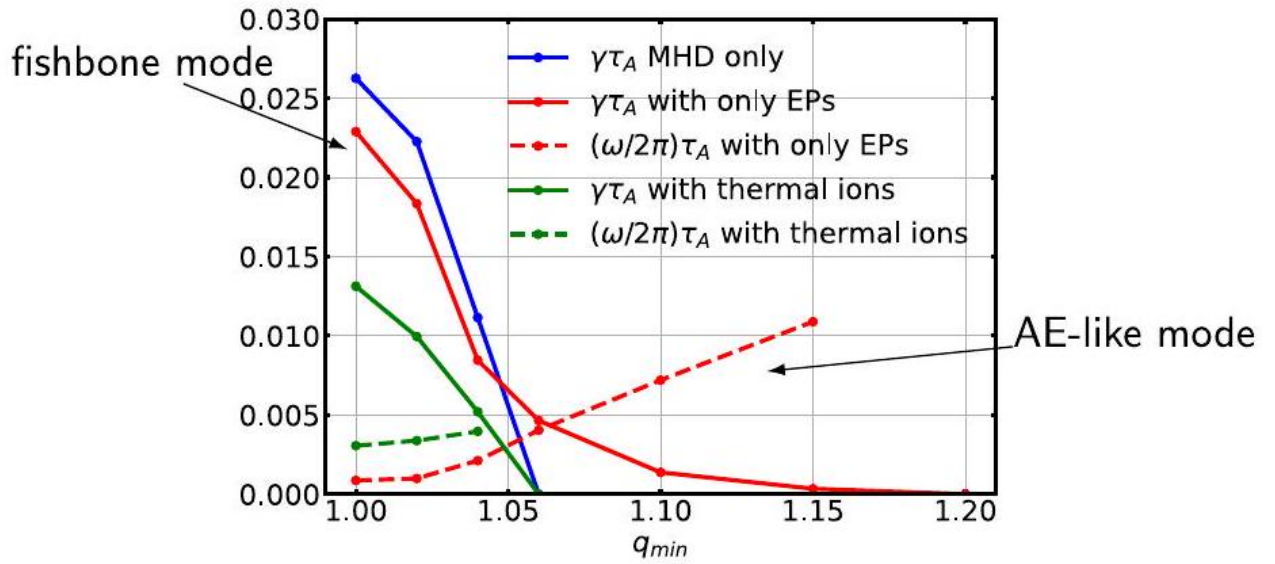


Figure 5: Growth rates (solid lines) and frequencies (dashed lines) as functions of q_{min} of the $n=1$ mode from M3D-C1 linear simulations with DIII-D equilibrium. The blue line shows the MHD-only result. The red lines show the kinetic-MHD results with only fast ions. The green lines show the results with both thermal and energetic ions.

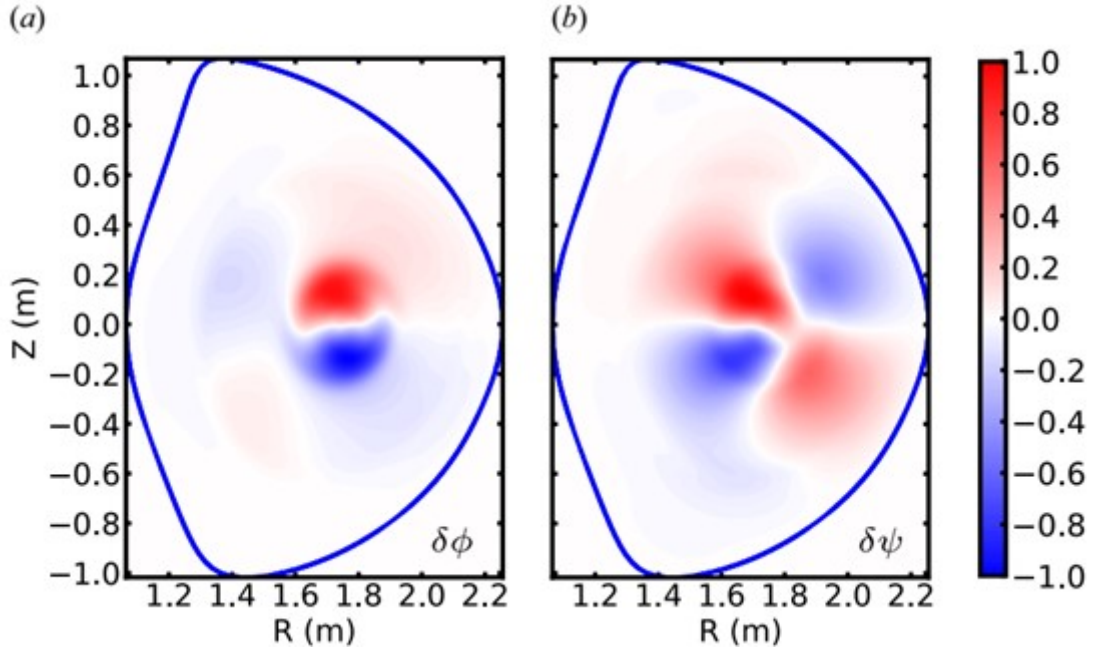


Figure 6: Two-dimensional structure of $\delta\phi$ (a) and $\delta\psi$ (b) from DIII-D $n = 1$ linear simulation of the $q_{\min} = 1.04$ case with thermal ions.

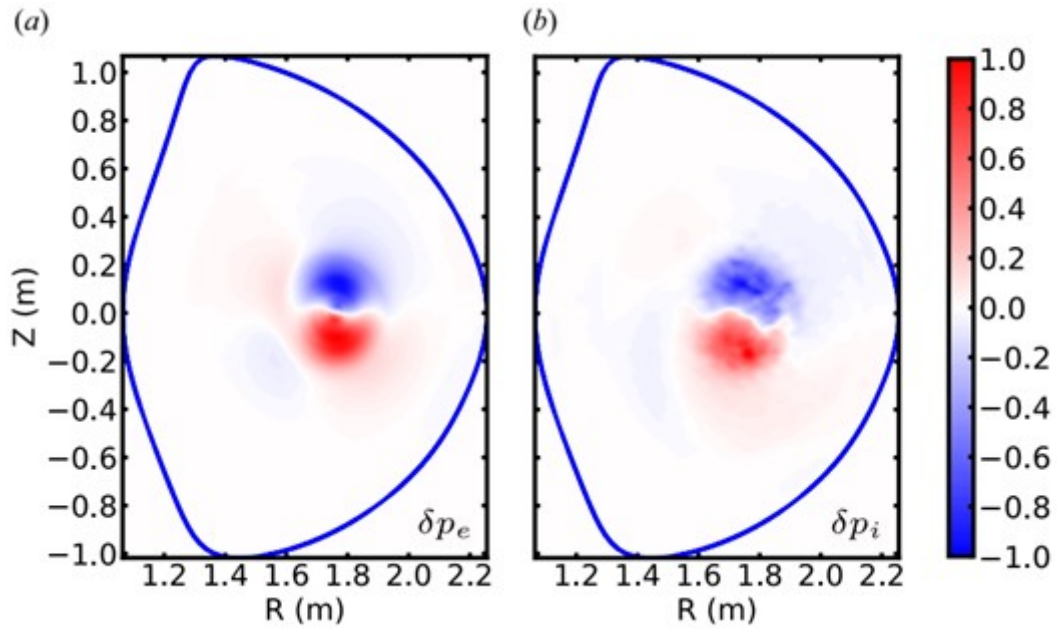


Figure 7: Two-dimensional structure of perturbed electron pressure δp_e (a) and thermal ion pressure δp_i (b) from the linear simulation of the $q_{\min} = 1.04$ case with thermal ions.

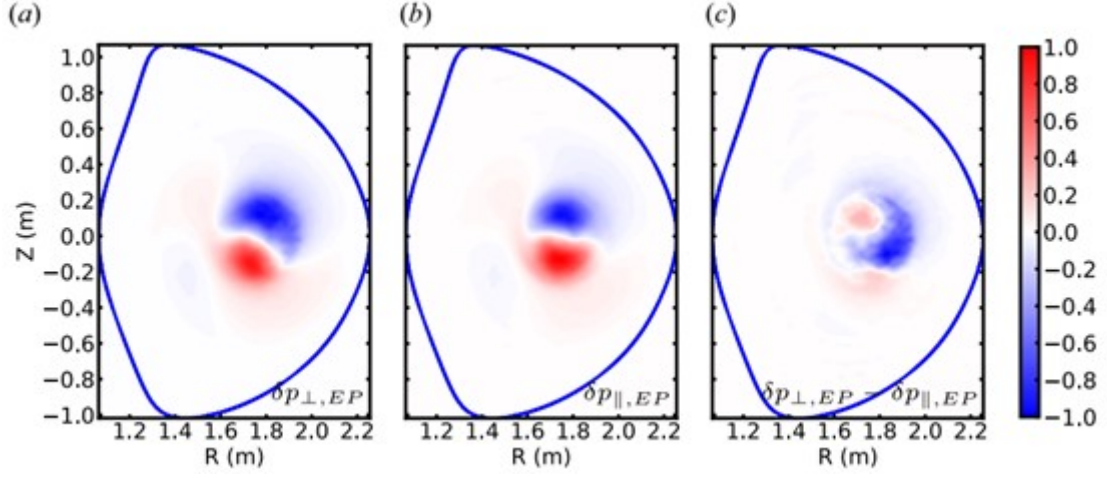


Figure 8: Two-dimensional structure of perpendicular (a) and parallel (b) fast ion pressure from the linear simulation of the $q_{\min} = 1.04$ case with thermal ions, and the difference between the two (c).

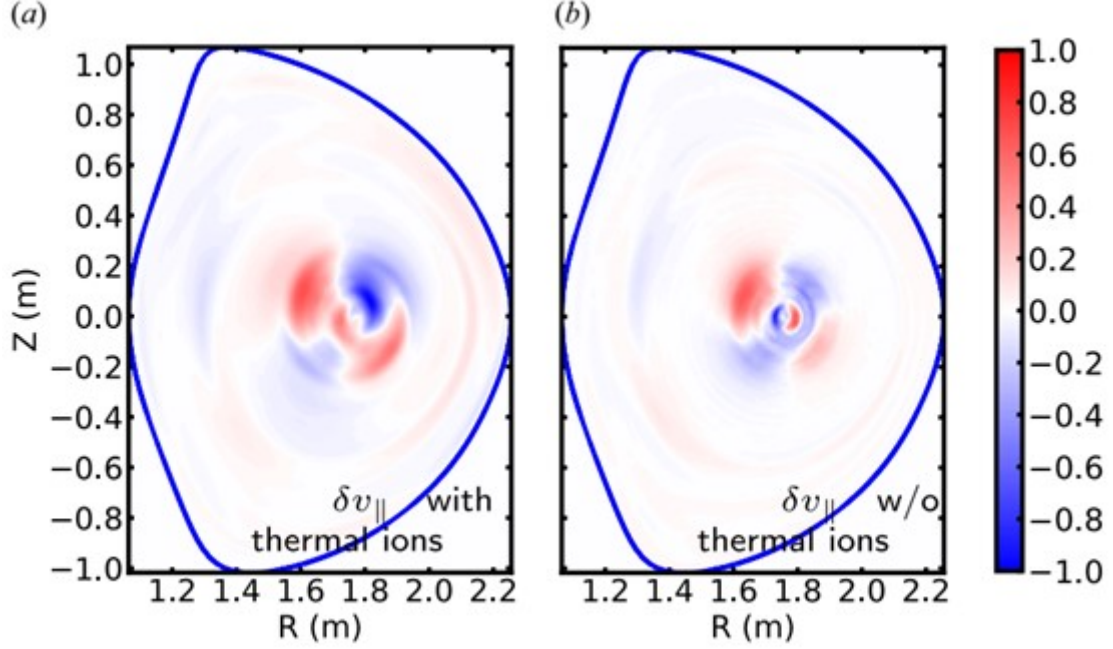


Figure 9: (a) Structure of v_{\parallel} from the linear simulation of the $q_{\min} = 1.04$ case with thermal ions and synchronization of $v_{\parallel}(2.20)$. (b) Structure of v_{\parallel} from the linear simulation with only fast ions using the MHD equation (2.23).

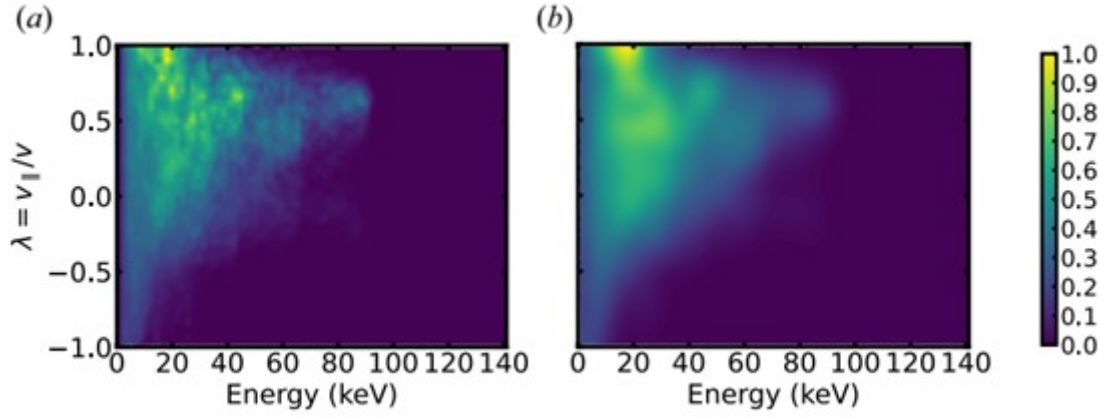


Figure 12: (a) The original EP distribution of energy and pitch angle near the magnetic axis from NUBEAM. (b) The smoothed EP distribution that was used in M3D-C1-K simulations.

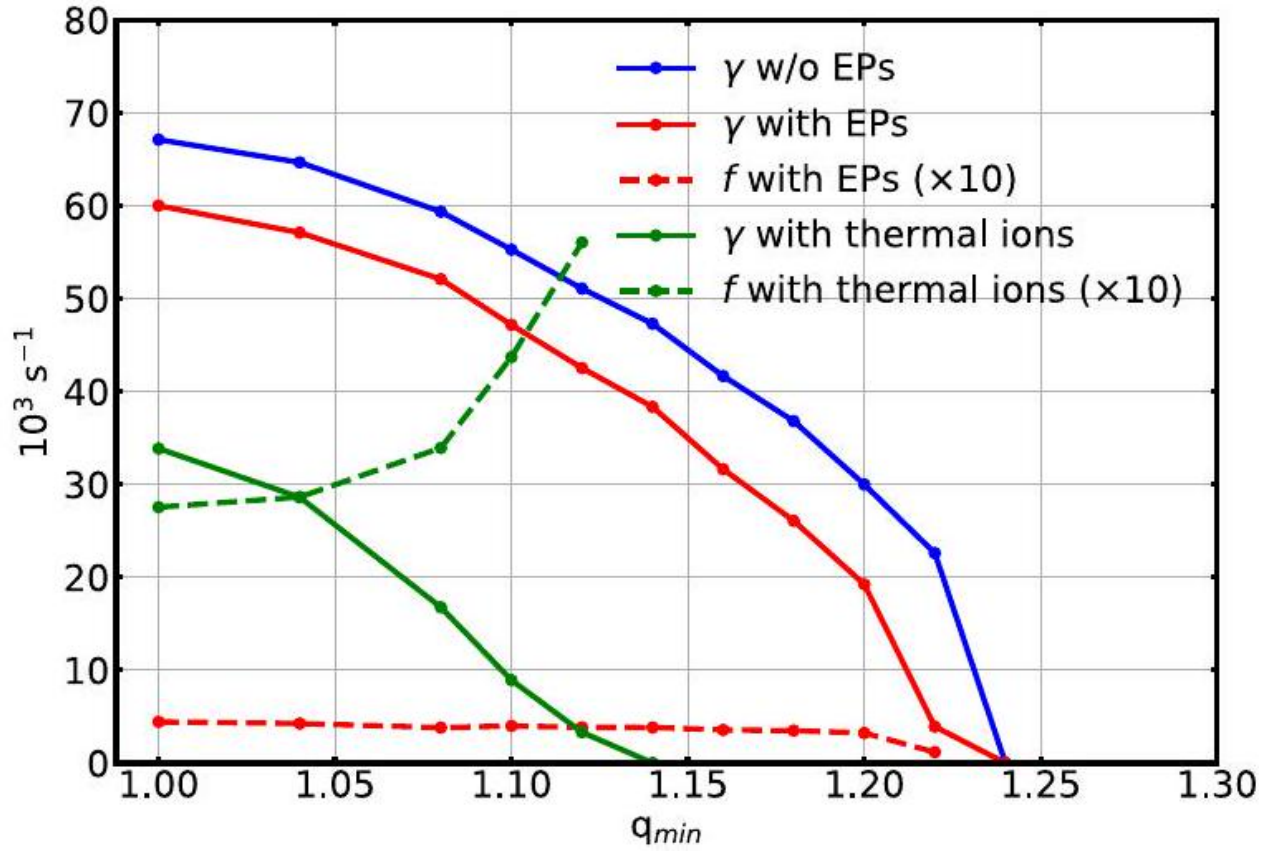


Figure 13: Growth rates γ (solid lines) and frequencies f (dashed lines) as functions of q_{min} of the $n = 1$ modes from M3D-C1 linear simulation with NSTX equilibrium with fixed β . The blue line shows the MHD-only result. The red lines show the kinetic-MHD results with only fast ions. The green lines show the results with both thermal and energetic ions.

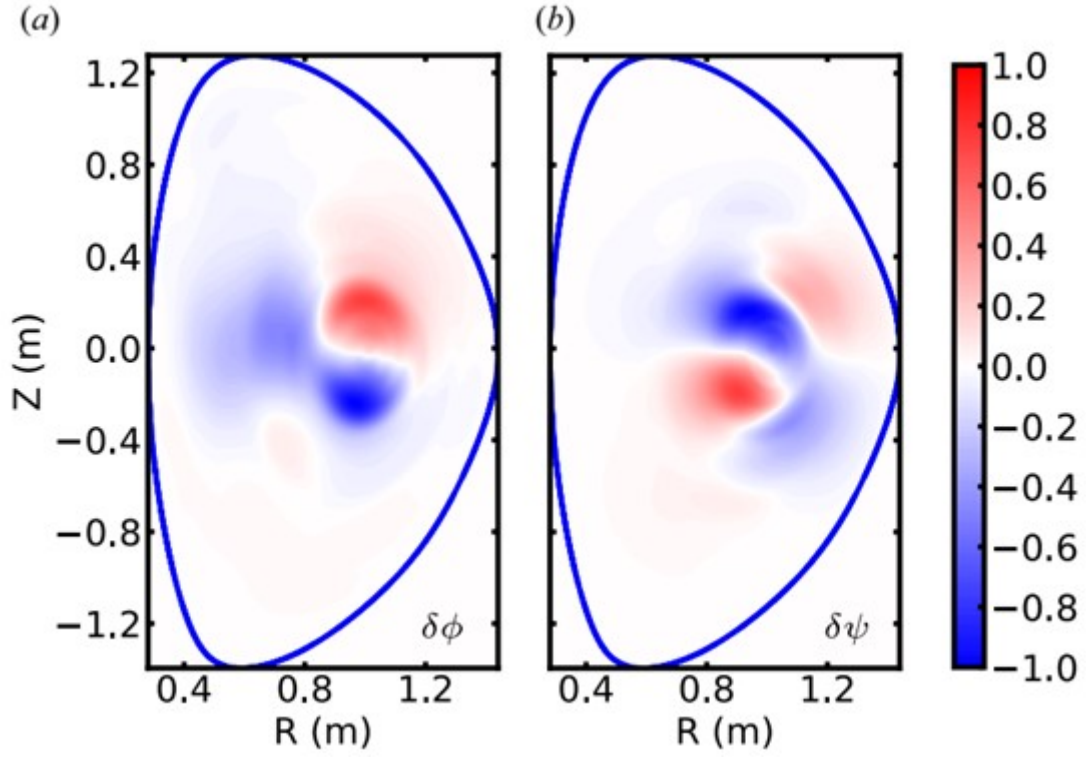


Figure 14: Two-dimensional structure of $\delta\phi$ (a) and $\delta\psi$ (b) from NSTX $n = 1$ linear simulation of the $q_{\min} = 1.08$ case with thermal ions.

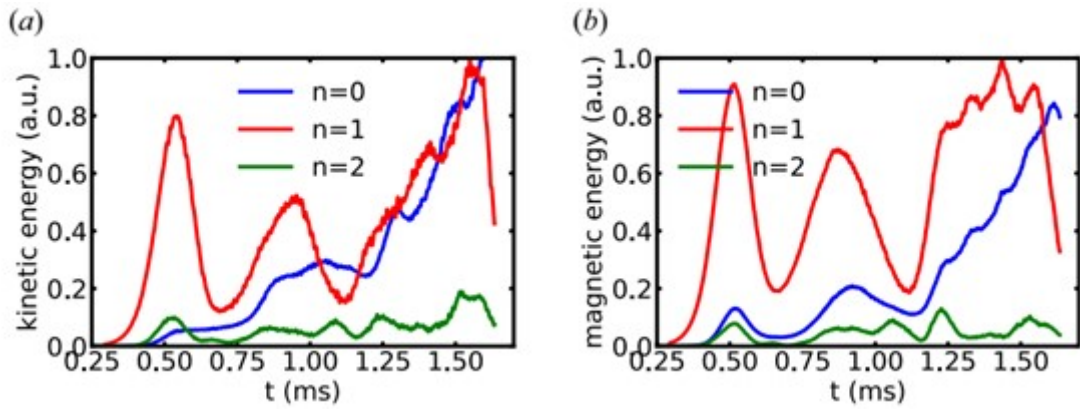


Figure 15: Time evolution of kinetic energy (a) and magnetic energy (b) of different toroidal harmonics from NSTX nonlinear simulation of the $q_{\min} = 1.08$ case with thermal ions.

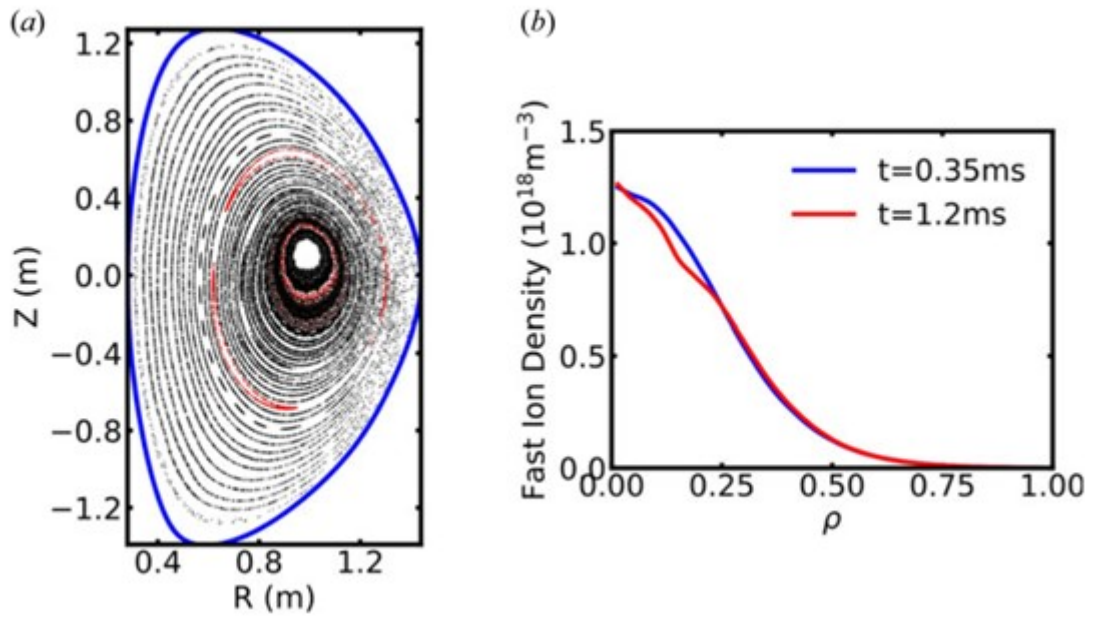


Figure 16: (a) Poincaré plot of magnetic flux surfaces at $t = 1.2$ ms. The (1,1) and (2,1) islands are marked as red. (b) Change of fast ion density profile in the nonlinear simulation of $q_{\min} = 1.08$ due to mode excitation.